Journal of the Society of Automotive Engineers Malaysia
Volume 3, Issue 2, pp 157-176, May 2019
e-ISSN 2550-2239 & ISSN 2600-8092

Controller Development for Magneto-Rheological Semi-Active Suspension System to Improve Vehicle Safety

M. S. F. Mansor[1,2*], H. Zamzuri[2], N. H. F. Ismail[1], A. A. Puad[3], M. Z. Che Mustafar[1], N. Abu Husain[3,4], L. Mohd Anuar[3], Z. Zainuddin[1], S. A. Mazlan[2] and A. N. Mohd Jahari[2,5]

[1]Active Safety, Safety Engineering, Group Engineering, Perusahaan Otomobil Nasional Sdn. Bhd.
[2]Vehicle System Engineering, Malaysia Japan International Institute of Technology, Universiti Teknologi Malaysia
[3]Advanced Engineering, Group Engineering, Perusahaan Otomobil Nasional Sdn. Bhd.
[4]School of Mechanical Engineering, Faculty of Engineering, Universiti Teknologi Malaysia
[5]Faculty of Electrical and Electronic Engineering Technology, Universiti Teknikal Malaysia Melaka

[*]*Corresponding author: shuhaim@proton.com*

ORIGINAL ARTICLE **Open Access**

Article History:

Received
20 Sep 2018

Received in revised form
10 Apr 2019

Accepted
12 Apr 2019

Available online
1 May 2019

Abstract – *Vehicle suspension system would complement vehicle safety in terms of ride comfort, handling and braking, and also isolation from road irregularities. This can be better achieved by introducing a semi-active suspension system where the magneto-rheological (MR) fluid is used to manipulate its damping characteristics. This paper explains the controller development for MR semi-active suspension system. The process started by developing the non-parametric linearized data driven (NPLDD) double input with proportional-integral (PI) controller as an inner loop algorithm for MR damper modelling and force tracking control; then, Improved PI controller as an outer loop control algorithm for vehicle response improvement, and finally validation work using quarter-car test bench. All the algorithm development is based on Perusahaan Otomobil Nasional (PROTON) vehicle characteristics and specifications. From the simulation results, it is verified that the NPLDD double input model together with the PI control strategy has the capability to track the desired damping force well. Meanwhile, the Improved PI controller for the outer loop is capable to reduce the magnitude of vehicle body acceleration and displacement. The validation at the quarter-car test bench also shows significant reduction of these two parameters. As a result, the PI controller for the MR semi-active suspension system is found sufficient for vehicle safety improvement.*

Keywords: Magneto-rheological damper, NPLDD double input, PI controller, force tracking control, inner loop and outer loop, semi-active suspension system

Journal homepage: www.jsaem.saemalaysia.org.my

1.0 INTRODUCTION

A damper is a device that dissipates energy in the form of heat. Energy is changed to heat by forcing a viscous fluid through an orifice. In a vehicle, energy from the road, rather than being transmitted to the vehicle, is changed into a temperature rise of the fluid inside of the damper. In this study, the damper is newly designed based on the configuration of the magneto-rheological approach as a control element for damper characteristics. In order to achieve the design concept, *MR* fluid and controller to control the electric current are introduced instead of oil or gas that conventionally used in passive suspension. When the current is applied, the *MR* fluid will be exposed to the magnetic field, and thus the iron particle will be changed into chain-like structure, as in Figure 1. The changes of iron particles in *MR* fluid will influence the changes in shear stress and viscosity of the fluid in less than 10 ms. As a result, the suspension will become more or less stiff (Imaduddin et al., 2013). This paper containing a brief explanation about the *MR* damper in section Introduction, *MR* damper modeling by using NPLDD double method and the usage of PI controller as an inner loop algorithm for *MR* damper modelling and force tracking control in section Materials and Methods, the application of Improved PI controller as an outer loop control algorithm for vehicle response improvement and the validation of controller for both inner and outer loop by using quarter-car test bench in section Results and Discussions, and conclusion in last section.

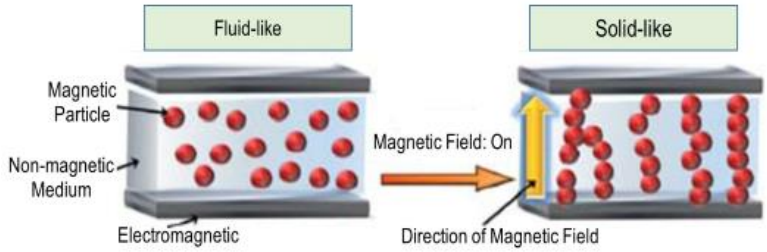

Figure 1: Iron particle of *MR* fluid (Bong et al., 2010)

1.1 *MR* Damper

As described in previous chapter, the most popular application of *MR* fluid is *MR* damper, which has been commercially applied in various high-end cars to provide an adjustable suspension (Carlson & Jolly, 2000) and a semi-active suspension (Sabino et al., 2011).

1.1.1 MR Damper Design

The performance of *MR* damper is basically depended on the efficiency of a valve that is usually located inside the piston. There are several types of *MR* valve systems had been designed such as annular-type, radial-type, and the combination of annular and radial valves (Fitrian et al., 2014). Among several designs for *MR* valves, Yoo and Wereley (2002), Ai et al. (2006), and Wang et al. (2009) were successfully developed *MR* valves less than 50 mm diameter with an achievable pressure drop of more than 1.5 MPa at 40 ml s−1 flow rate. Based on that, Imaduddin et al. (2015) have proposed a design based on multiple annular and radial valves in order to improve the achievable pressure drop of an *MR* valve.

Figure 2 shows the innovative approach for the proposed design that is a valve with a meandering flow path. Thus, the total effective area in an *MR* valve was increased without compromising the size and power requirement of the valve. This approach is further enhanced

the pressure drop of the valve due to meandering flow path process allows the *MR* fluid to undergo magnetization several times inside the valve (Fitrian et al., 2014).

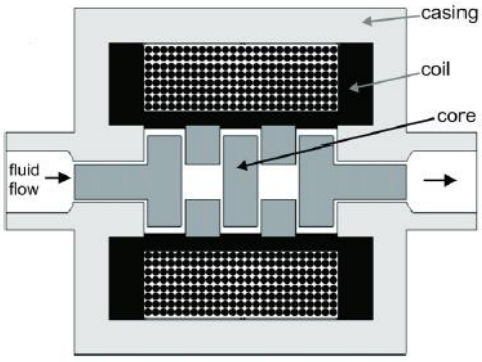

Figure 2: Basic concept of the *MR* valve with a meandering flow path (Fitrian et al., 2014)

1.1.2 Propose MR Damper Working Principle

The schematic of *MR* damper is shown in Figure 3. The design of the newly *MR* damper consists of two cylinders where the air needs to fill in cylinder 2 in order to boost and maintain the output force of *MR* damper. Based on the valve design, the *MR* fluid can be manipulated in order to control the *MR* damper. The working principle of this *MR* damper is much similar to the existing damper in the market, except the damping characteristic can be controlled. At zero current, the *MR* damper is acting as a normal vehicle damper system. When sealed piston exhibits an external force, the sealed piston will traverse back and forth inside cylinder 1. If the sealed piston in cylinder 1 is compressed, the *MR* fluid will flow through *MR* valve to accumulator and feed back to cylinder 1 again via bypass channel. If the piston in cylinder 1 is extended, the *MR* fluid will flow through *MR* valve from accumulator and feed back to cylinder 2 via bypass channel.

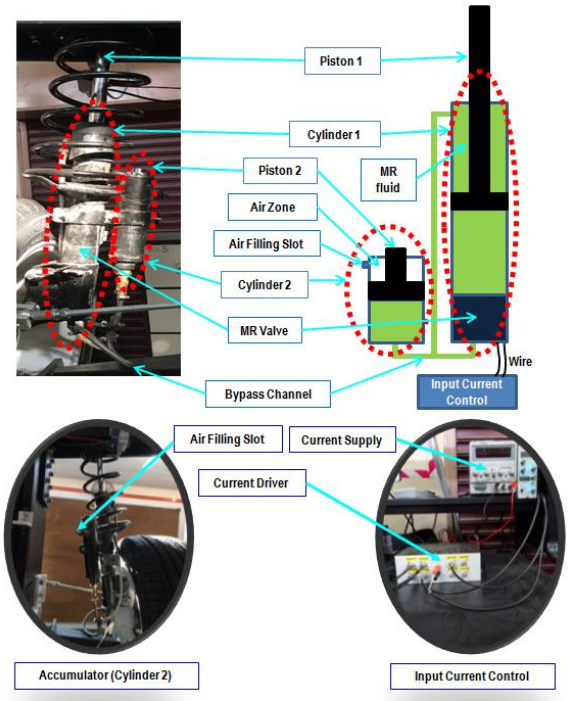

Figure 3: *MR* damper schematic diagram

The piston in cylinder 2 is used to separate the *MR* fluid and air. Here, there is one slot located at the top of cylinder 2 to be used to fill in the air. The slot can be covered and tightened-up by shielded screw. The air is used to accommodate the change in the *MR* fluid cylinder volume. As the piston rod in cylinder 1 compresses, the air compresses to compensate for the change in volume available to the *MR* fluid. When the piston rod in cylinder 1 is extending, the air expands in order to avoid the creation of a vacuum. These working principles are applicable to all conditions even though the current varies.

2.0 MATERIALS AND METHODS

2.1 *MR* Damper Modelling

2.1.1 Proposed MR Damper Performance

MR damper has high non-linear dynamic behavior that needs an appropriate control algorithm in order to ensure the effectiveness of the system (Jansen & Dyke, 2000; Stutz & Rochinha, 2005). Hence, many researchers have conducted comprehensive study to design the control method of *MR* damper (Cha et al., 2014). For the proposed *MR* damper, when no electric current applied, the viscosity of *MR* fluid remains at 0.112 Pa-s. Then, the current was tuned slowly from 0.05 A, 0.25 A, 0.50 A, 0.75 A, and 1.00 A, the viscosity of MR fluid is expected to change and thus adjust the shear stress (force). The performance of *MR* damper was displayed in Figure 4(a) for *MR* damper force, Figure 4(b) for force-velocity, and Figure 4(c) for force-displacement. The graphs were plotted based on experimental data produced by Shimadzu machine, at 0.1 Hz of frequency and 10 mm suspension stroke length.

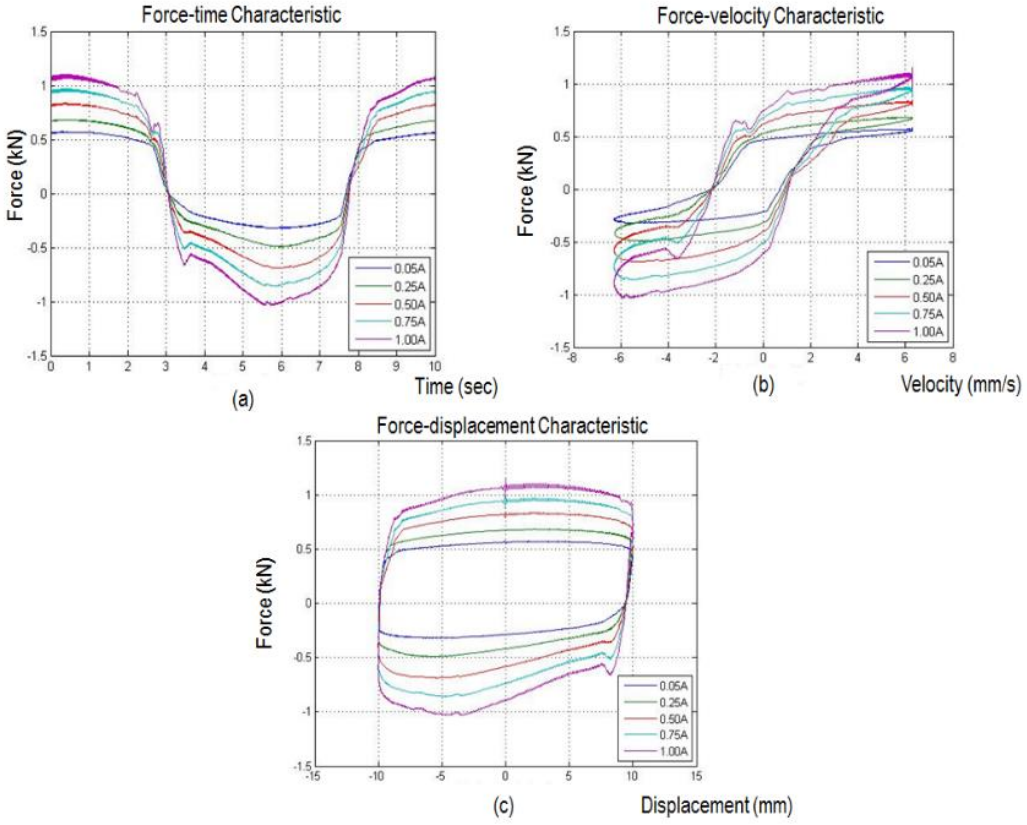

Figure 4: (a) Force, (b) Force-velocity and (c) Force-displacement graph of *MR* damper

Figure 4(a) – (c) show the highest damping force of the *MR* damper is ± 1 kN at 1 A and the lowest is ± 0.5 kN at 0.05 A. It can be concluded that, as the current increase, the damping force versus time, velocity, and displacement pattern increased. In other words, as the viscosity of *MR* fluid is increased, the *MR* damper will become stiffer or vice versa. Therefore, the suspension becomes less comfort but improves the handling and cornering.

The finding shows that the proposed *MR* damper – force, force-velocity and force-displacement pattern agree with the establish *MR* damper. The hysteresis behaviour was recorded similarly as Sabino et al. (2011), Hudha (2005), Mohd Samin (2010), Abu Bakar (2009, 2013), Harun et al. (2014) and Mohd Amin (2016). The force of *MR* damper was observed approximately 1 kN at maximum electric current, which is slightly lower compared to the nominal damping force required for the vehicle suspension system. The actual damping force for vehicle suspension system required 6 kN at 1.5 m/s of nominal suspension speed (Arifin et al., 2011, 2012). However, for the mean of controller design, the specification of existing proposed *MR* damper is adequate.

2.1.2 Proposed MR Damper Modelling

Several models have been proposed in order to model the dynamic behavior of the *MR* dampers. These include polynomial models (Choi et al., 2001; Du et al., 2005), a neural network model (Chang & Zhou, 2002), and phenomenological models built on the Bouc-Wen hysteretic model (Dyke et al., 1996). *MR* damper can be modelled based on parametric and non-parametric approaches. Example of parametric approaches is the Bingham model, Bouc-Wen model, non-linear viscoelastic-plastic model, and others. While examples for the non-parametric approach is non-parametric linearized data driven single input approach, non-parametric linearized data driven double input approach, simple polynomial approach, and others. The *MR* damper model development can be classified as an inner loop where the controller also needs to be designed for damping force tracking. In this study, the non-parametric model is selected to represent the *MR* damper. Except its simplicity, robustness, and widely used by many researchers, the proposed technique also had been selected because the model was configured properly to represent the physical damper characteristics, such as hysteresis and force saturation. Song et al. (2005) found that the non-parametric model could capture reliable *MR* damper than the parametric model to greatly improve numerical efficiency. Furthermore, the non-parametric models can be predicted, thus easy to develop real-time advanced control algorithm due to its fast-numerical speed and differentiability.

Among the non-parametric model type, the NPLDD techniques were selected for further analysis to represent the *MR* damper. The NPLDD was opted due to its simplicity of an algorithm and no optimisation method involved in model development. The NPLDD technique is divided into two types which are NPLDD single input and NPLDD double input. Furthermore, these two types of *MR* damper modelling are capable to follow the S-shape function of the force-velocity curve. Thus, the optimisation tool is eliminated for the modelling development in order to predict the optimum parameters of the mathematical function (Hudha, 2005). In order to build an easy-for-implementation *MR* damper model for both simulation and real-time control systems, the proposed modelling approach is developed based on the experimental data. Generally, the approach involves five main steps. The first step is the investigation of force-velocity curve of *MR* damper conducted via experimental works. The applied current is set to 0.05 A with an increment of 0.05 A until 1.00 A. The cyclic motion is set to 0.1 Hz. The second step is obtaining the hard points of experimental data from step one as illustrated in Figure 5. The hysteresis loop of each force-velocity curve is divided into two

regions namely the positive (upper loop or compression) and negative acceleration (lower loop or extension) (Sabino et al., 2011). The hard points are selected in every incisive bend of both upper and lower curves in order to capture the non-linear characteristic of *MR* damper (Hudha, 2005). The damper force is linearly interpolated if the real-time damper velocity lies in between the two vectors of input values using the following interpolation formula:

$$f = f_i + \frac{dv - dv_i}{dv_{i+1} - dv_i}(f_{i+1} - f_i) \quad (1)$$

where $f_i < f < f_{i+1},\ dv_i < dv < dv_{i+1}$ and i is the i^{th} vector of both input and output values.

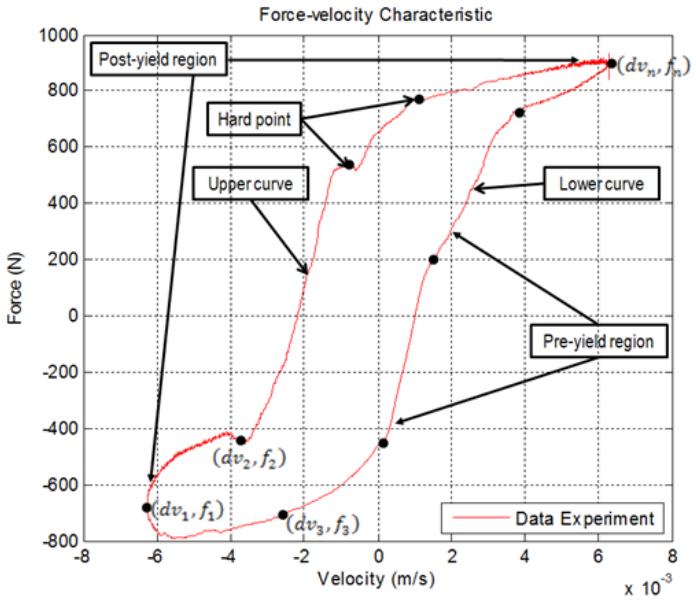

Figure 5: Hard points taken from the experimental result

In each subsystem, the hard points of experimental data are mapped in the form of a look-up table for a set of applied electric current signals. In the fourth step, the damper force is linearly interpolated if the electric current signal applied to the model lies between the specified input signals. Finally, the output of the model namely the damper force is selected by a switch block. The switch block will pass through the output of positive acceleration subsystem if the acceleration of the damper is greater or equal to zero. Otherwise, the switch block will pass through the output of negative acceleration subsystem.

2.1.3 Proposed MR Damper Validation

The findings for both force-velocity and force-displacement are presented in Figure 6 for NPLDD method respectively. In this case, the current value is set to 0.55 A.

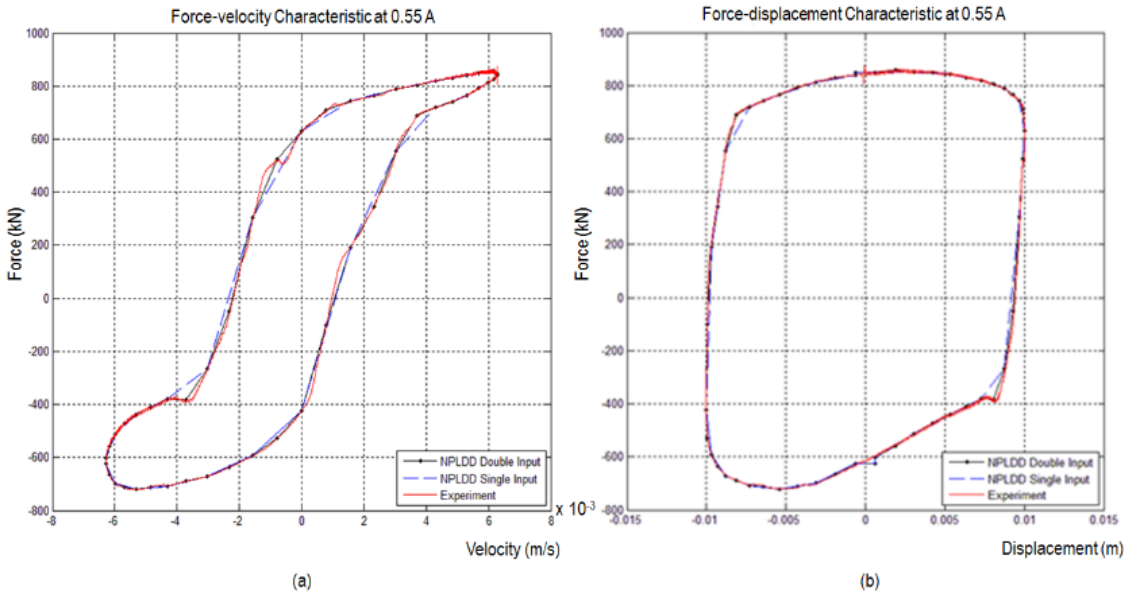

Figure 6: (a) Graph of force-velocity and (b) force-displacement characteristic of NPLDD model

It is interesting to note that in all cases of this study from Figure 6 clearly verified that the proposed model are in agreement with those obtained with the experimental data. Thus, this suggests that the methods are suitable for MR damper model. In addition, the root mean square error (RMSE) value for each method was calculated by comparing with the experimental data and tabulated in Table 1 where the NPLDD double input revealed the lowest RMSE value. Thus, it can be concluded that NPLDD double input is the most suitable method to represent the *MR* damper model.

Table 1: RMSE value for the proposed method of *MR* damper modeling

Method	***RMSE* for Upper Curve (*N*)**	***RMSE* for Lower Curve (*N*)**
NPLDD Double Input	275.344	516.0233
NPLDD Single Input	311.0241	518.1807

2.1.4 Inner Controller of Proposed MR Damper

An effective *MR* damper model is expected to be comparable to the prototype and easy to control. The inner controller of *MR* damper or force tracking control is used as a control strategy to ensure that the actual damping force equal to the required force by the suspension. This is to guarantee that the cabin comfort can be increased. In this control strategy, the actual damping force of *MR* damper is fed back and compared with desired force. The resulting error is controlled using PI controller where the corrected signal is then converted to electric current. The electric current is then triggered the respective suspension velocity to produce the actual damping force. Figure 7 depicts the controller diagram for inner block.

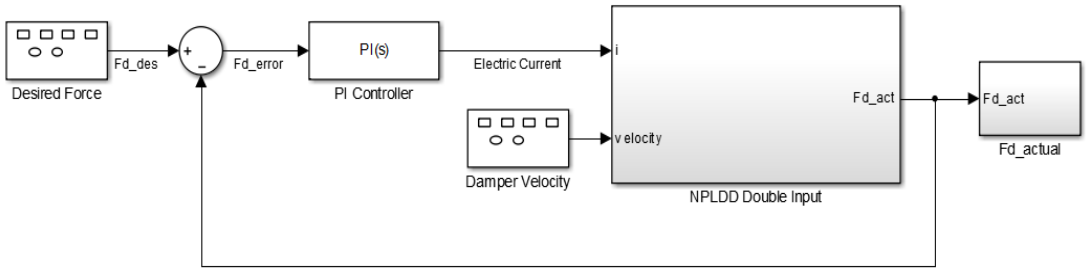

Figure 7: Controller diagram for inner block

In order to ensure the actual damping force is following the desired damping force, the PI controller was tune systematically. The algorithm of tuning is based on the mathematical expression given as follows:

$$u(t) = K_p e(t) + K_i \int e(t) \tag{2}$$

$$e(t) = F_{d_{des}}(t) - F_{d_{act}}(t) \tag{3}$$

where K_p is a proportional gain, K_i is an integral gain, e is an error, $F_{d_{des}}$ is a desired damping force, and $F_{d_{act}}$ is an actual damping force of *MR* damper. In this simulation, the parameter of K_p and K_i are set to be 1500 and 100 respectively, where these values are determined by trial and error method. Figure 8 presents the simulation results for sine, square, and saw-tooth wave function respectively.

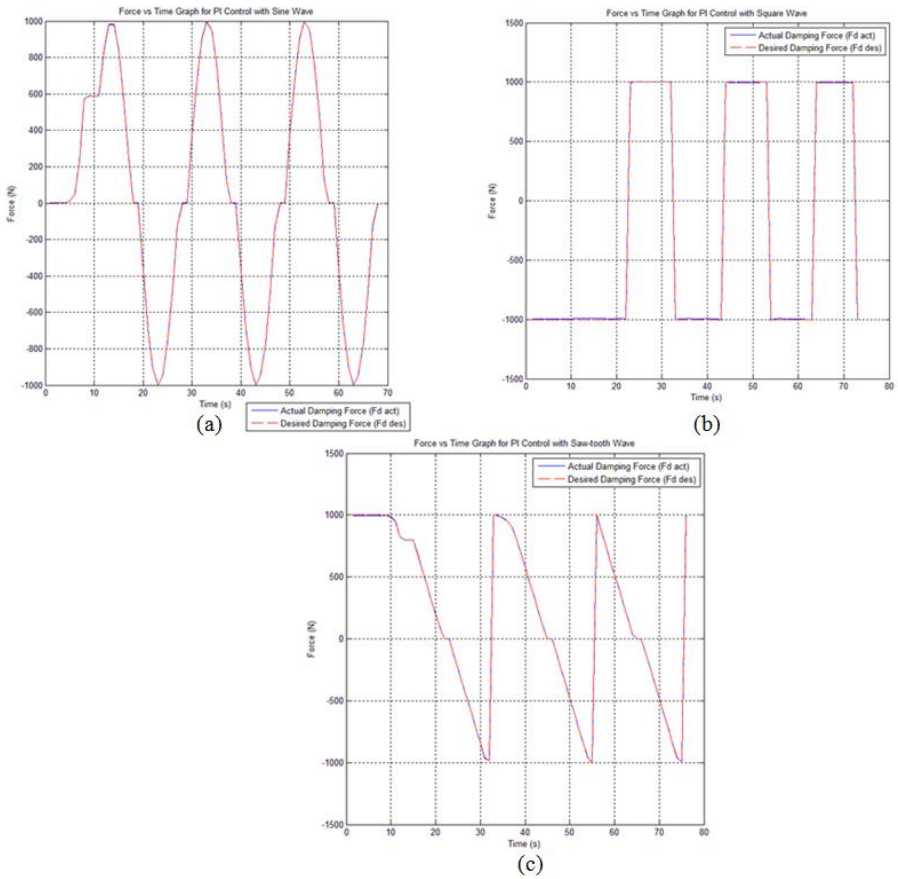

Figure 8: Force tracking of PI control for (a) sine wave, (b) square wave and (c) saw-tooth wave

The accuracy and validity of the *NPLDD* double input model was also demonstrated by comparing the force prediction error at various applied electric current signals. The present result for the controllability of the proposed model was verified using PI control strategy to track desirable damping force. The *RMSE* value for *PI* controller exhibit almost 100% similar to an input which is sine, square, and saw-tooth wave respectively. The results of this investigation show that the proposed *MR* damper model tracks the desired force.

3.0 RESULTS AND DISCUSSION

3.1 The Application of *Pi* Controller for Vehicle Suspension System

The development of quarter-car vehicle model is necessary to design simplified model undergoing suspension maneuver to evaluate the performance of the control system. The quarter-car vehicle model will be used for system analysis and computer simulation. This development model is based on application of Newton's second law equation to wheel and vehicle dynamics to get the motion equation. The complete mathematical model of the quarter vehicle model is derived based on the approach presented in Mansor et al. (2012). The mathematical expression is used to develop vehicle model for the purpose of the controller design. The equation is established by many researchers to represents the vehicle dynamic behavior of the vehicle system (Sabino et al., 2011; Abu Bakar, 2009, 2013; Sam & Hudha, 2006). The vehicle model is applied to the plant block of the closed-loop system as depicts in Figure 9.

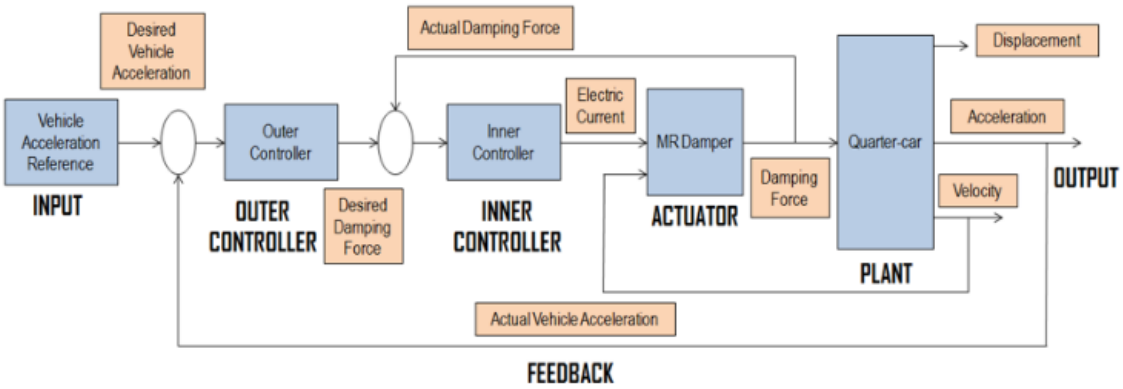

Figure 9: Block diagram of the control strategy

The quarter-car model parameters are described in Table 2. The parameters are based on PROTON Prevé suspension specification (Arifin et al., 2011, 2012) and also from Hudha (2005).

Table 2: Parameter for quarter-car simulation model

Parameter	Symbol	Value	Unit
Mass of vehicle body / Sprung mass	M_b / M	290	kg
Mass of suspension / Un-sprung mass	M_w / m	59	kg
Suspension spring stiffness	C_S / c_S	16,812	N/m
Suspension damping	D_S / d_S	1,000	N/m/s
Tire spring stiffness	K_t / k_t	190,000	N/m

The test performed in this simulation is to ride over bump and pothole. The quarter-car moves forward at a constant speed and crosses the bump before hit the pothole that is positioned crosswise with the quarter-car's direction of travel. The tire will cross the bump at time $t = 2\text{s}$ and hit the pothole at time $t = 8\text{s}$. The vertical motions of tire will be transferred to the quarter-car body resulting in vertical motions of the body. Figure 10 shows the bump and pothole geometry and quarter-car's forward speed of bump and pothole test.

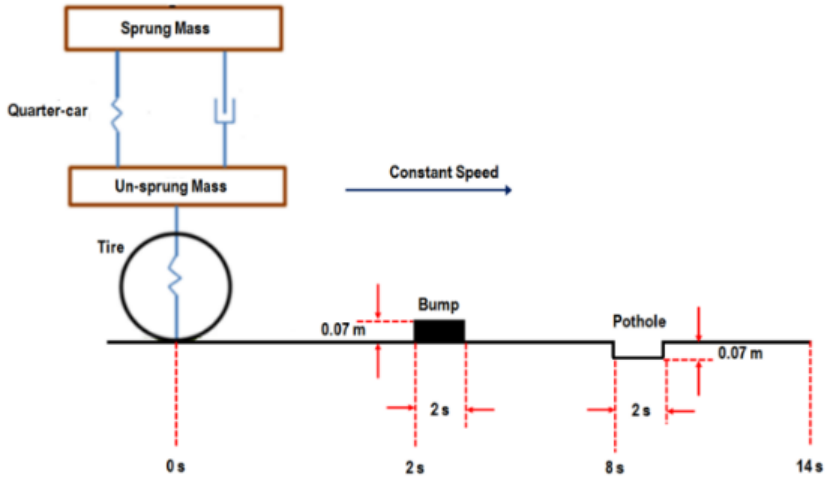

Figure 10: Bump and pothole test

Generally, the testing should include the sport and comfort mode to obtain the performance of the suspension system. The comfort-mode is defined as cabin comfort when the acceleration of the vehicle body is equal to zero, while the sport-mode is defined as sporty performance when the vehicle is attached the road input profile. In other words, the comfort-mode is for ride quality and sport-mode is for handling purposes. In this study, the comfort mode is concentrated due to its reasonable for the ride quality assessment. In addition, the quarter-car model with 2 degree-of-freedom (DOF) is suitable to present the characteristic of comfort mode. The quarter-car response for observation is quarter-car body displacement (z_B), body acceleration $(\ddot{z}_B)$, suspension deflection (SD), and tire load (TL). The performance of the controller is determined by comparing the magnitude of the output vehicle response with the passive system. The percentage of reduction also is calculated to obtain the ride quality improvement. Root-mean-square (*RMS*) is the most suitable measurement parameter to observe the comparison. *RMS* is defined as a continuously varying function in terms of integral of the squares of the instantaneous values during a cycle.

The controller development consists of outer controller design and evaluation to ensure the output response is reacting as much as possible as per input reference, as in Figure 10. In this study, for the ride quality assessment, the input is set to zero for the vehicle acceleration reference. This is because; the cabin comfort is exhibit when no movement inside the vehicle cabin since the suspension is absorbed all the force towards the vehicle body. Thus, all the controllers are needed to tune until the acceleration approximately equals to zero. The controllers involved in this study are Improved *PI* controller. It had been identified as "Improved" controller due to the additional control algorithm before the proposed controllers. This control algorithm is known as the sprung mass velocity modification, as shown in Figure 11, is needed to improve the damping force. Thus, the cabin comfort can be further improved

during the quarter-car exhibit the bump and pothole of road input phenomenon.

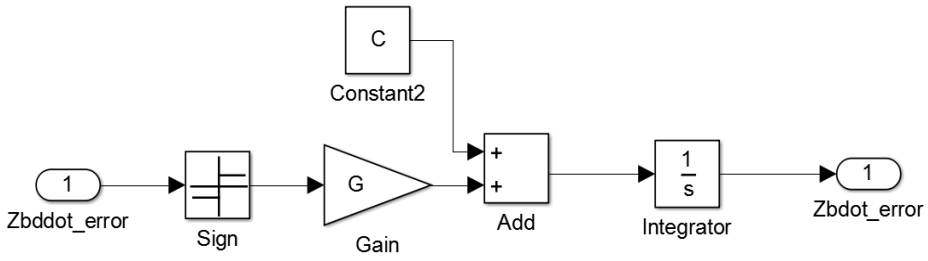

Figure 11: Sprung mass velocity modification

The sprung mass velocity error (z_{bdot_error}) modification is obtained from the acceleration feedback from the quarter-car model. The error of sprung mass acceleration (z_{bddot_error}) can be calculated by comparing the actual acceleration (z_{bddot_actual}) from quarter-car model and desired acceleration ($z_{bddot\_desired}$). The equation of the modification process is depicted as:

$$\ddot{z}_{b\_\text{error}} = \ddot{z}_{b\_\text{desired}} - \ddot{z}_{b\_\text{actual}} \tag{4}$$

$$\dot{z}_{b\_\text{error}} = \int \left(G.sgn.\ddot{z}_{b\_\text{error}}\right) + C \tag{5}$$

where G is the damping gain and set to 1,000 and C is the damping constant which is set to 1,500. The sgn function, as in Equation (5), is used to allow the acceleration of sprung mass error signal to be processed for the next stage if the magnitude of desired and actual acceleration is in the same direction. Else, the acceleration is set to zero. Then, the acceleration of sprung mass error signal is converted to the velocity of sprung mass error signal. Since the reference or desired input is set to zero due to ride comfort setting, the Equation (4-5) can be rewritten as:

$$\ddot{z}_{b\_\text{error}} = -\ddot{z}_{b\_\text{actual}} \tag{6}$$

$$\dot{z}_{b\_\text{error}} = \int -\left(G.sgn.\ddot{z}_{b\_\text{actual}}\right) + C \tag{7}$$

where Equation (7) is used for the *PI* controller strategy design. Figure 12 displays the *PI* controller to generate the corresponding desired control force for the *MR* damper and Figure 13 shows the details block diagram for all entire systems.

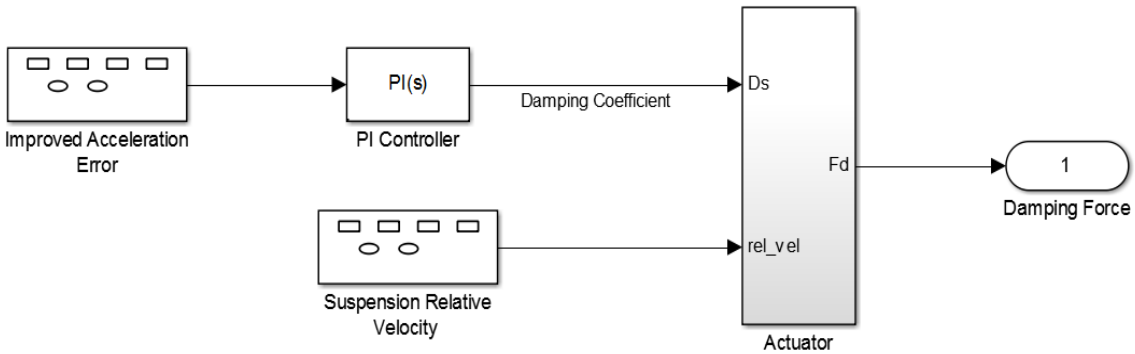

Figure 12: Block diagram for PI controller algorithm

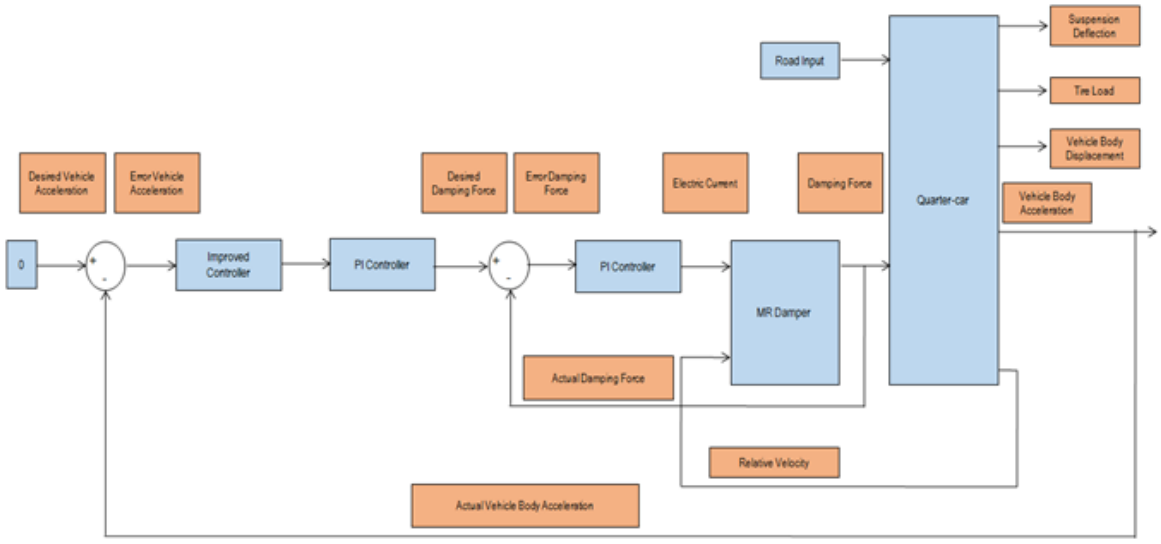

Figure 13: Overall block diagram for Improved PI controller

In order to produce sufficient damping force to decrease the magnitude of the ride quality of quarter-car for cabin comfort, the *PI* controller needs to tune systematically. The algorithm of tuning is based on the mathematical expression given as:

$$u(t) = K_p e(t) + K_i \int e(t) + K_d \frac{d}{dt} e(t) \tag{8}$$

where $K_d = 0$,

$$e(t) = \ddot{z}_{B_{des}}(t) - \ddot{z}_{B_{act}}(t) \tag{9}$$

where $\ddot{z}_{B_{des}}$ is a desired suspension acceleration, and $\ddot{z}_{B_{act}}$ is an actual suspension acceleration of quarter-car. In this simulation, the parameter of K_p and K_i are set to be 0.798 and 0.00998 respectively, where these values are determined by trial and error method. The observation is performed by comparing it with passive suspension system. Figure 14 and Figure 15 are shown the vehicle output response of ride quality for the quarter-car system that is using Improved *PI* controller algorithm.

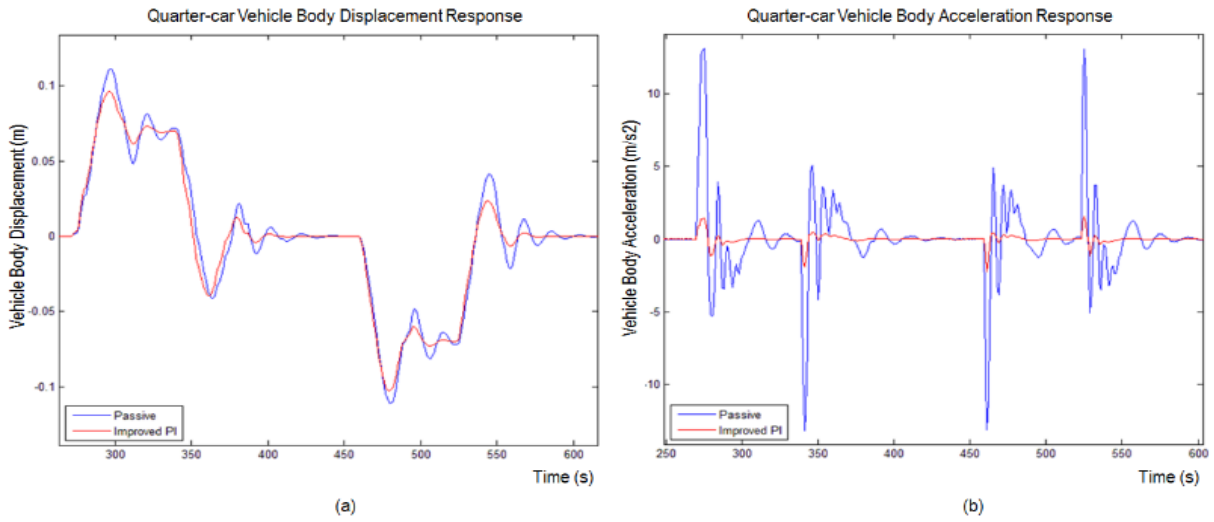

Figure 14: Quarter-car body (a) displacement and (b) acceleration output response for Improved PI controller

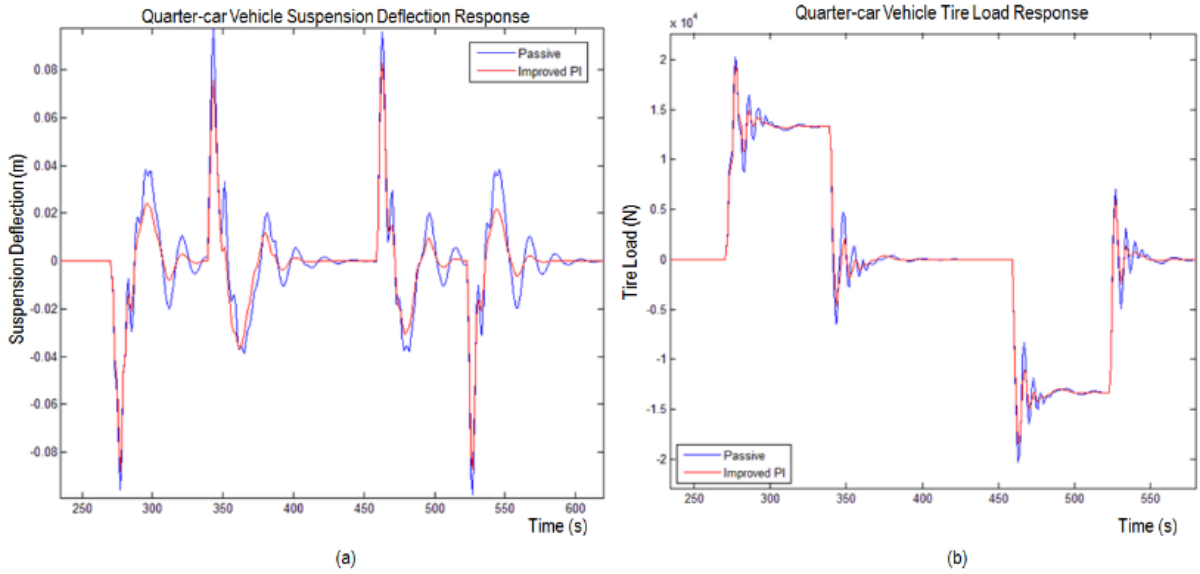

Figure 15: Quarter-car (a) suspension deflection and (b) tire load output response for Improved PI controller

From Figure 14 and Figure 15, it can be observed that the controlled algorithm is described as a better response compared to passive system. In addition, the *RMS* value was calculated between controlled and passive to determine the effectiveness of the controller algorithm, as shown in Table 3.

Table 3: RMS value for output vehicle response for Improved PI controller

Quarter-car Response	*RMS*		Percentage of Reduction (%)
	Passive	Improved *PI*	
Body displacement (m)	0.03528	0.03379	4.21
Body acceleration (m/s^2)	2.08624	0.25719	87.67
Suspension deflection (m)	0.01785	0.01487	16.67
Tire load (N)	6,270.80	6,227.60	0.68

From Table 3 above, it can be concluded that the Improved *PI* controller is able to reduce the vehicle output response for all entire comfort parameters especially body acceleration by 87.67%. Thus, the Improved *PI* controller is suitable to be used to maximize vehicle cabin comfort.

3.2 Controller Validation Using Quarter-Car Test Bench

A quarter-car test bench is a simulation of one suspension system of a vehicle. The bench consists of tyre, spring, damper, mass which represent weight of the vehicle, hydraulic system for road input simulation, *dSPACE* software, current controller box, supply voltage, and wire harness. The *dSPACE* software is used for hardware communication. The controller (inner and outer loop) algorithm that deployed in *dSPACE* software will give an input (electric current) to the current controller box to supply to the *MR* damper. The signal is in Pulse Width Modulation (PWM) format where the pulse is transmitting out from the *dSPACE*.

Current controller box will receive the pulse and translate to the voltage signal. The voltage signal needs to convert the signal to the electric current. It can be achieved by adding a resistor to convert the voltage drop to the current flow. The full system of *MR* damper suspension system in quarter-car test bench is shown in Figure 16.

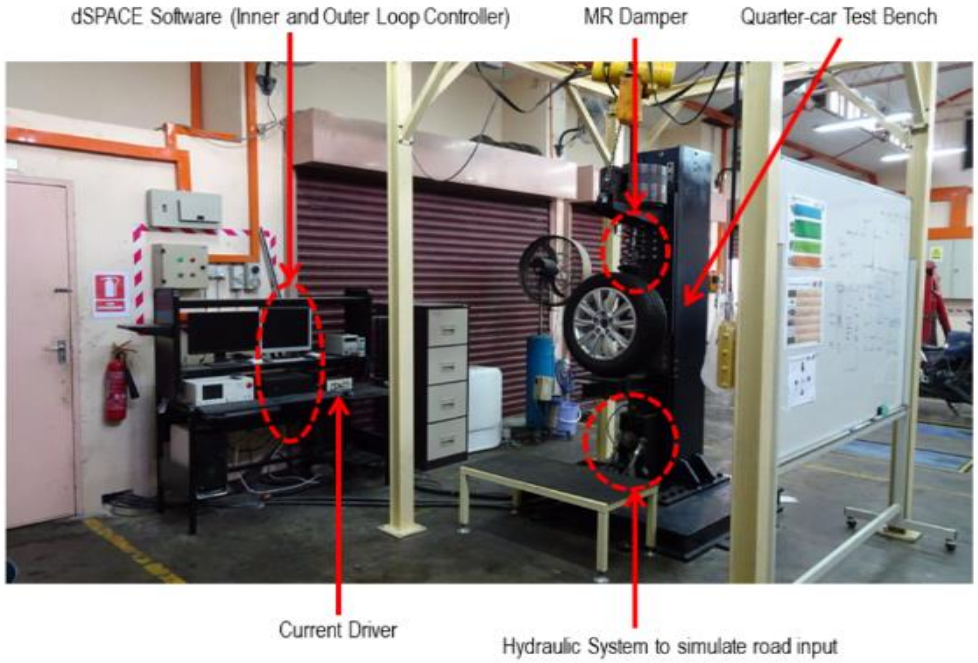

Figure 16: Complete quarter-car test bench for MR damper suspension system

The complete controller algorithm for the inner and outer loop controller that is deployed in *dSPACE* software is shown in Figure 17. The *MR* damper that is already integrated into quarter-car test bench can be evaluated and tested accordingly.

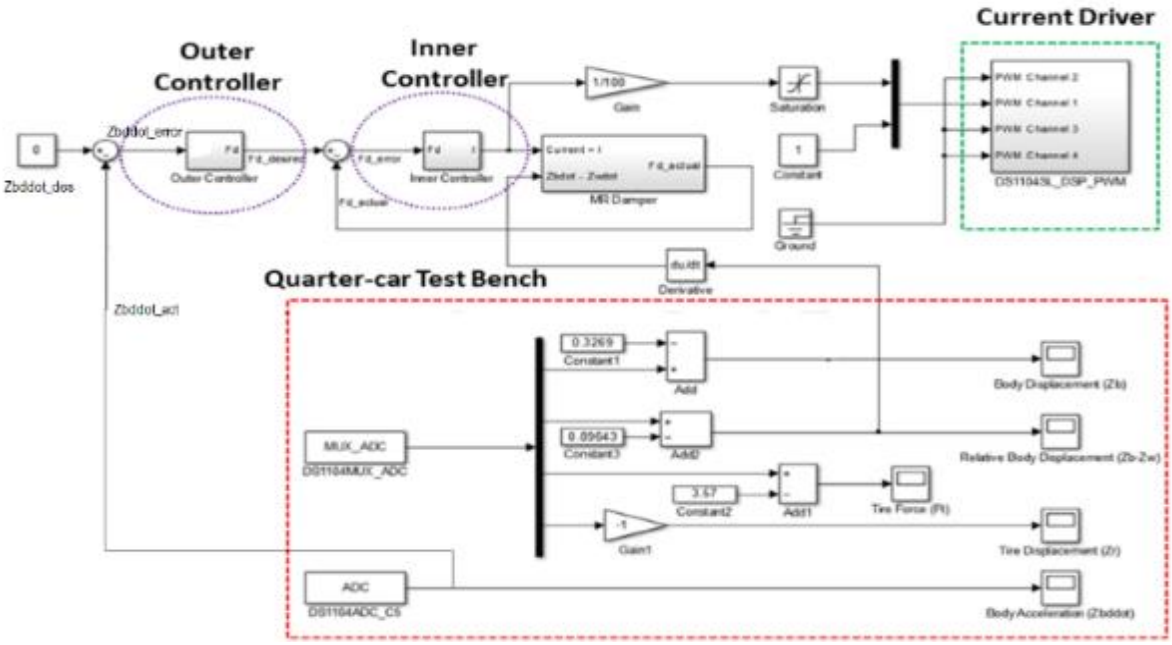

Figure 17: Algorithm in dSPACE for outer and inner loop controller

After deploying the controller block into the *dSPACE*, the evaluation can be executed. The hydraulic system is used to simulate the road input where it can be set as rectangle, sine, and triangle wave. In this research, the rectangle wave is using since it can represent the bumper and pothole pattern. There is electric current change observed during the evaluation. Therefore, the controller is confirmed to be working well since the required electric current can be supplied according to road input. The response of vehicle state is shown in Figure 18 and 19 below.

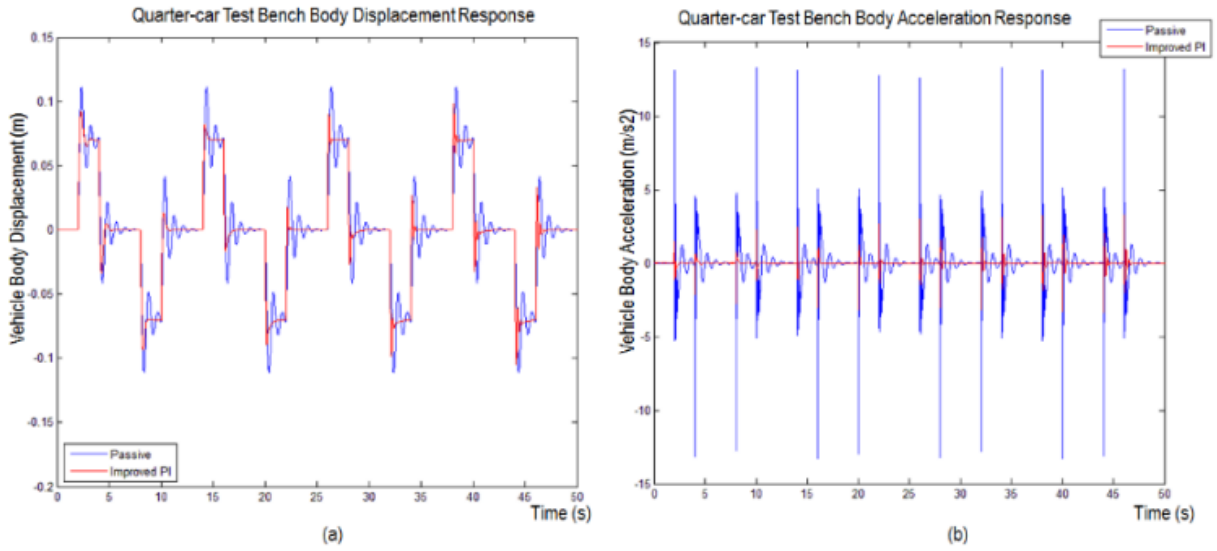

Figure 18: Quarter-car test bench body (a) displacement and (b) acceleration output response for Improved PI controller

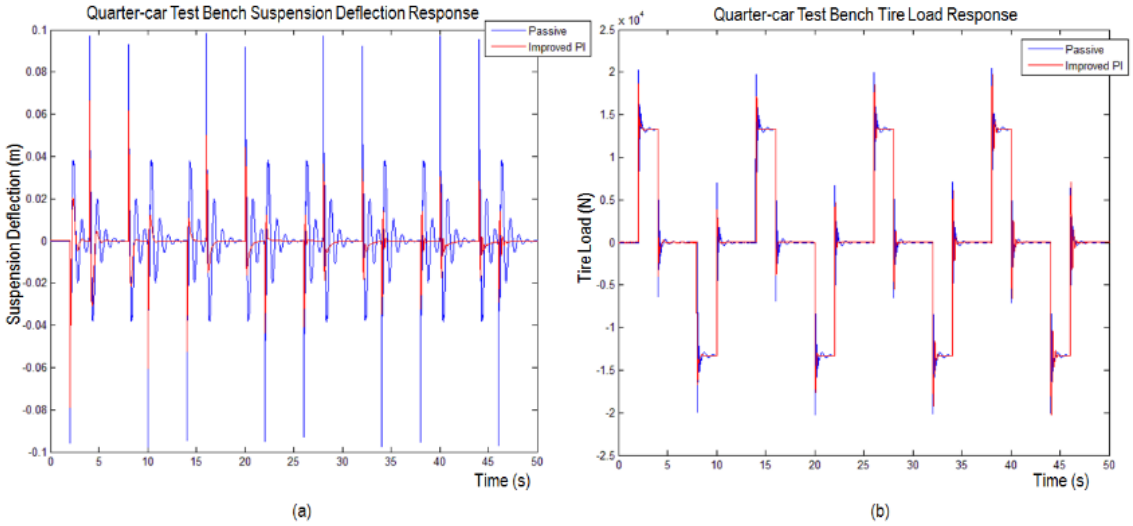

Figure 19: Quarter-car test bench (a) suspension deflection and (b) tire load output response for Improved PI controller

The response of the vehicle state shows the significance difference as per target after the controller had been applied. In addition, the *RMS* value was calculated between controlled and passive to determine the effectiveness of the controller algorithm, as shown in Table 4.

Table 4: RMS value for output quarter-car test bench response for Improved PI controller

Quarter-car Test Bench Response	*RMS*		Percentage of Reduction (%)
	Passive	Improved *PI*	
Body displacement (m)	0.04131	0.03919	5.09
Body acceleration (m/s^2)	2.31527	0.29091	87.44
Suspension deflection (m)	0.01851	0.01497	19.13
Tire load (N)	7,375.96	7,236.34	1.89

From Table 4 above, it can be concluded that the Improved *PI* controller is able to reduce the quarter-car test bench output response for all entire comfort parameters especially body acceleration by 77%. Thus, the Improved *PI* controller is suitable to be used to maximize vehicle cabin comfort. In addition, as a controller validation, it shows a similarity of output response between the simulation in *MATLAB* and quarter-car test bench, as per in Table 5 and Table 6 below.

Table 5: RMS value for MATLAB and quarter-car test bench simulation for the output vehicle response for passive

Output Response	*RMS* Passive		Percentage of Similarity (%)
	MATLAB	Quarter-car Test Bench	
Body displacement (m)	0.03528	0.04131	85.40
Body acceleration (m/s^2)	2.08624	2.31527	90.11
Suspension deflection (m)	0.01785	0.01851	96.43
Tire load (N)	6,270.80	7,375.96	85.02

Table 6: RMS value for MATLAB and quarter-car test bench simulation of vehicle response by using Improved PI controller

Output Response	*RMS* Improved *PI*		Percentage of Similarity (%)
	MATLAB	Quarter-car Test Bench	
Body displacement (m)	0.03379	0.03919	86.22
Body acceleration (m/s^2)	0.25719	0.29091	88.41
Suspension deflection (m)	0.01487	0.01497	99.33
Tire load (N)	6,227.60	7,236.34	86.06

From Table 5 and 6 above, it can be concluded that the *MATLAB* and quarter-cat test bench is shown 85% and above of similarity for all entire comfort parameters either for passive or Improved *PI* controller of suspension system.

4.0 CONCLUSION

The proposed *NPLDD* model for the damping force of *MR* damper has been investigated in this study. The measured experimental damping force was compared with the predicted ones the proposed model. It has been demonstrated that the proposed model agrees well the non-linear behaviour hysteresis behaviour of the *MR* damper in the form of force-velocity characteristics. The advantages of the proposed model are in the use of a simple algorithm and do not need a length numerical optimisation for parameter estimation. In addition, the controllability of the proposed model was investigated in both simulation and experimental works by realising a simple closed-loop control namely PI control. The *PI* controller is sufficient to control the actual output to track to the desired input as an inner loop and the actual quarter-car acceleration for outer loop. From simulation study, it can be seen clearly that under several input functions, the *NPLDD* double input model tracks the desired damping force well for inner loop and minimize the quarter-car output response for outer loop. The Improved *PI* controller is functioning well for outer loop control where the output response especially vehicle body acceleration, vehicle body displacement, suspension deflection, and tire load had shown a significant improvement compared to passive system. Furthermore, the validation of the controller in quarter-car tests bench shows high percentage of similarity as a simulation in *MATLAB*. This improvement will lead the vehicle exhibit more comfort and thus will affect the vehicle safer.

ACKNOWLEDGEMENTS

This research is supported by Perusahaan Otomobil Nasional Sdn. Bhd. (PROTON), Ministry of Higher Education and the Universiti Teknologi Malaysia (UTM) through the internal research grant Vot: 4C099 by Assoc. Prof. Ir. Dr. Saiful Amri Mazlan. The authors are grateful to the PROTON and UTM for supporting the present work. In addition, the authors are appreciative of PROTON Management, Mr. Hazrin Fazail Haroon as Head of Group Engineering for encouraging all engineers to write and submit a technical paper for knowledge-sharing purposes. The author would like to thanks Ir. Azmi Osman as Head of Advanced Engineering, Ir. Mohd Marzuki Abdul Majid as Head of Computer-Aided Engineering, and Hj. Razman Che Rose as Vehicle Chief Engineer for their effort of reviewing this paper.

REFERENCES

Abu Bakar, S.A. (2009). *Modeling and control of magnetorheological damper in semi-active suspension system of passenger vehicle* (MEng thesis). UTM.

Abu Bakar, S.A. (2013). *Magnetorheological semi active suspension employing semi-active damping force estimator algorithms for passenger vehicle* (PhD thesis). UTM.

Ai, H.X., Wang, D.H., & Liao, W.H. (2006). Design and modeling of a magnetorheological valve with both annular and radial flow paths. *Journal of Intelligent Material Systems and Structures, 17*, 327-334.

Arifin, S.N., Rahim, M.F., & Long, A.W. (2011). *P321A PP stage suspension specification release.* Perusahaan Otomobil Nasional Sdn. Bhd. (PROTON).

Arifin, S.N., Rahim, M.F., & Long, A.W. (2012). *P321A P1 stage objective vehicle dynamics measurement.* Perusahaan Otomobil Nasional Sdn. Bhd. (PROTON).

Bong, J.P., Fei Fei, F., & Hyoung, J.C. (2010). Magneto-rheology: Materials and application. *The Royal of Chemistry*, *6*, 5246-5253.

Carlson, J.D., & Jolly, M.R. (2000). *MR* fluid, foam, and elastomer devices. *Mechatronics, 10***,** 555-569.

Cha, Y., Agrawal, A.K., Friedman, A., Phillips, B., Ahn, R., Dong, B., Dyke, S.J., Spencer, B.F., Ricles, J., & Christenson, R. (2014). Performance validations of semi-active controllers on large-scale moment-resisting frame equipped with 200-kN MR damper using real-time hybrid simulations. *Journal of Structural Engineering*, 140(10), 04014066. doi: 10.1061/(ASCE)ST.1943-541X.0000982

Chang, C.C., & Zhou, L. (2002). Neural network emulation of inverse dynamics for a magnetorheological damper. *Journal of Structural Engineering*, *128*(2), 231-239.

Choi, S.B. Lee, S.K., & Park, Y.P. (2001). A hysteresis model for the field-dependent damping force of a magneto-rheological damper. *Journal of Sound and Vibration*, *245*(2), 375-383.

Du, H., Sze, K.Y., & Lam, J. (2005). *Semi-active H∞ control of vehicle suspension with magneto-rheological dampers. Journal of Sound and Vibration*, *283*, 981-996.

Dyke, S.J., Spencer Jr., B.F., Sain, M.K., & Carlson, J.D. (1996). Modeling and control of magneto-rheological dampers for seismic response reduction. *Smart Materials and Structures*, *5*, 565-575.

Fitrian, I., Saiful Amri, M., Mohd Azizi, A.R., Hairi, Z., Ubaidillah, S., & Burhanuddin, I. (2014). A high performance magnetorheological valve with a meandering flow path. *Smart Materials and Structures*, *23*(6), 1-21. 065017. doi: 10.1088/0964-1726/23/6/065017

Harun, M.H., Ahmad, F., Md Yunos, M.R., & Mat Yamin, A.K. (2014). Non-parametric modelling and validation of magnetorheological damper for lateral suspension of railway vehicle using interpolated sixth order polynomial. *Applied Mechanics and Materials*, *699*.

Hudha, K. (2005). *Non-parametric modelling and modified hybrid skyhook groundhook control of magneto-rheological dampers for automotive suspension system* (PhD thesis). UTM.

Imaduddin, F., Mazlan, S.A., & Zamzuri, H. (2013*).* A design and modeling review of rotary magneto-rheological damper. *Material and Design*, *51*, 575–591. https://doi.org/10.1016/j.matdes.2013.04.042

Imaduddin, F., Mazlan, S. A., Zamzuri, H., & Yazid, I.I.M. (2015). Design and performance analysis of a compact magnetorheological valve with multiple annular and radial gaps. *Journal of Intelligent Material Systems and Structures*, *26***,** 1038-1049.

Jansen, L.M., & Dyke, S.J. (2000). Semi-active control strategies for MR dampers: A comparative study. *ASCE Journal of Engineering Mechanics*, *126*(8), 795-803.

Mansor, M.S.F., Syed Eddy, A.S.A., Alias, A., Zainul Abidin, M.A., & Zamzuri, H. (2012). *Adaptation of linear electric motor into vehicle suspension system.* Paper presented at 2012 Japanese Society of Automotive Engineers (JSAE) Annual Congress, Yokohama, Japan.

Mohd Samin, P. (2010). *Hybrid stability augmentation system-force control of semi-active suspension with magneto-rheological damper* (PhD thesis). UTM.

Mohd Amin, M.H.I. (2016). *Development of external orifice semi-active suspension system (EOSASS) for armored vehicle* (MSc thesis), UPNM.

Sabino, U., Hudha, K., Akmar, F., & Kadir, A. (2011). Modelling, characterisation, and force tracking control of a magnetorheological damper under harmonic excitation. *International Journal of Modeling Identification and Control*, *13*(1/2), 9-21.

Sam, Y.M., & Hudha, K. (2006). *Modelling and force tracking control of hydraulic actuator for an active suspension system.* Paper presented at 2006 1st IEEE Conference on Industrial Electronics and Applications, Singapore.

Song, X., Ahmadian, M., & Southward, S. (2005). Modeling magnetorheological dampers with application of nonparametric approach. *Journal of Intelligent Material Systems and Structures*, 16(5), 421-432.

Stutz, L.T., & Rochinha, F.A. (2005). *A comparison of control strategies for magneto-rheological vehicle suspension systems*. Paper presented at XII International Symposium on Dynamic Problems of Mechanics, Ilhabela, SP, Brazil.

Wang, D.H., Ai, H.X., & Liao, W.H. (2009). A magnetorheological valve with both annular and radial fluid flow resistance gaps. *Smart Materials and Structures*, *18*, 115001.

Yoo, J.H., & Wereley, N.M. (2002). Design of a high-efficiency magnetorheological valve. *Journal of Intelligent Material Systems and Structures, 13***,** 679-685.

Appendix I. Abbreviations and Notations

MR	-	Magneto-rheological
NPLDD	-	Non-parametric linearized data driven
PROTON	-	Perusahaan Otomobil Nasional
RMSE	-	Root mean square error
PI	-	Proportional-integral
K_p	-	Proportional gain
K_i	-	Integral gain
e	-	Error
$F_{d_{des}}$	-	Desired damping force
$F_{d_{act}}$	-	Actual damping force
M_b / M	-	Mass of vehicle body / sprung mass
M_w / m	-	Mass of suspension / Un-sprung mass
C_S / c_S	-	Suspension spring stiffness
D_S / d_S	-	Suspension damping
K_t / k_t	-	Tire spring stiffness
DOF	-	Degree-of-freedom
z_B	-	Quarter-car body displacement
$\ddot{z}_B$	-	Quarter-car body acceleration
SD	-	Quarter-car suspension deflection
TL	-	Tire load
RMS	-	Root-mean-square
z_{bdot_error}	-	Sprung mass velocity error
z_{bddot_error}	-	sprung mass acceleration error
z_{bddot_actual} / $\ddot{z}_{B_{act}}$	-	Actual quarter-car body acceleration
$z_{bddot\_desired}$ / $\ddot{z}_{B_{des}}$	-	Desired quarter-car body acceleration
G	-	Damping gain
C	-	Damping constant
sgn	-	Signum function
dSPACE	-	Repository software package
MATLAB	-	Matrix laboratory software
UTM	-	Universiti Teknologi Malaysia
PWM	-	Pulse Width Modulation